INTERNATIONAL JOURNAL FOR NUMERICAL METHODS IN FLUIDS
Int. J. Numer. Meth. Fluids 2007; **54**:1021–1030
Published online 11 April 2007 in Wiley InterScience (www.interscience.wiley.com). DOI: 10.1002/fld.1498

A Numerical model based on the mixed interface-tracking/interface-capturing technique (MITICT) for flows with fluid–solid and fluid–fluid interfaces

Marcela A. Cruchaga[1,*,†], Diego J. Celentano[2] and Tayfun E. Tezduyar[3]

[1]*Departamento de Ingeniería Mecánica, Universidad de Santiago de Chile (USACH), Av. Bdo. O'Higgins 3363, Santiago, Chile*
[2]*Departamento de Ingeniería Mecánica y Metalúrgica, Pontificia Universidad Católica de Chile, Av. V. Mackenna 4860, Santiago, Chile*
[3]*Mechanical Engineering, Rice University—MS 321, Houston, TX 77005, U.S.A.*

SUMMARY

We propose a numerical model for computation of flow problems that involve both fluid–solid and fluid–fluid interfaces. The model is based on the mixed interface-tracking/interface-capturing technique (MITICT), which was introduced earlier for problems that involve both fluid–solid interfaces that are accurately tracked with a moving mesh method and fluid–fluid interfaces that are too complex to track and therefore treated with an interface-capturing technique. In our numerical model, fluid–solid interfaces are handled with the moving Lagrangian interface technique (MLIT) and fluid–fluid interfaces with the edge-tracked interface locator technique (ETILT). The mixed technique is tested in computation of a fluid–particle interaction problem in the presence of a fluid–fluid interface impacted by the particle.

Received 23 January 2007; Revised 1 March 2007; Accepted 6 March 2007

KEY WORDS: fluid–solid interface; fluid–fluid interface; fluid–particle interaction; MLIT; ETILT; MITICT

1. INTRODUCTION

Computation of flow problems with fluid–solid and fluid–fluid interfaces poses a number of numerical challenges. One of the major challenges associated with fluid–solid interfaces is the accurate representation of the interface geometry and the corresponding boundary layer and nearby flow field. Interface-tracking (moving mesh) techniques, such as the arbitrary Lagrangian–Eulerian

*Correspondence to: Marcela A. Cruchaga, Departamento de Ingeniería Mecánica, Universidad de Santiago de Chile (USACH), Av. Bdo. O'Higgins 3363, Santiago, Chile.
†E-mail: mcruchag@lauca.usach.cl

Contract/grant sponsor: Chilean Council of Research and Technology CONICYT; contract/grant number: 1060141
Contract/grant sponsor: Department of Technological and Scientific Research at the University of Santiago de Chile (DICYT-USACH)

(ALE) methods (see, for example, [1–7]) and the deforming-spatial-domain/stabilized space–time (DSD/SST) formulation [8–11], meet this challenge. In these techniques, the mesh moves to follow the interface, providing the fine mesh resolution needed near the fluid–solid interface. A good number of finite element moving mesh techniques have been developed for computation of fluid–structure and fluid–particle interactions (see, for example, [12–21]). In computation of flow problems with very complex and unsteady fluid–fluid interfaces, interface-tracking techniques may require remeshing that is too frequent to be acceptable. In such cases, interface-capturing (non-moving mesh) techniques can be used as robust and economical solution methods, with the understanding that the accuracy near the interface will be limited by the mesh resolution where the interface happens to be located at a given instant. Using these interface-capturing techniques in computation of fluid–solid interfaces would limit the accuracy of the flow field near the solid surface to the accuracy one can get with the mesh resolution where the interface is.

The accuracy of the interface-capturing techniques near the interface can be increased to a limited extent, and this can be done in various ways. An example is the enhanced discretization interface-capturing technique (EDICT) [22], which was introduced for computation of free-surface and multi-fluid flows with enhanced discretization (and therefore increased accuracy) near the interface. Non-moving mesh techniques with such enhanced discretization or enrichment (see, for example, [23, 24]) were proposed for computation of fluid–solid interfaces. It is important to realize that methods based on such enhanced discretization or enrichment techniques would be hard pressed to resolve a boundary layer to the same extent that a moving mesh method can.

When a flow problem involves both fluid–solid and fluid–fluid interfaces, we can use a mixed method, so that each type of interface is handled with the technique most appropriate for that type of interface. The mixed interface-tracking/interface-capturing technique (MITICT) [16] was introduced with that in mind. In the MITICT, fluid–solid interfaces are accurately tracked with a moving mesh method, and fluid–fluid interfaces, if they are too complex and unsteady to track, are treated with an interface-capturing technique. The MITICT was successfully tested in [25], where the interface-tracking technique is the DSD/SST formulation, and the interface-capturing technique is the edge-tracked interface locator technique (ETILT) [16, 26, 27].

In the work presented here, for flow problems that involve both fluid–solid and fluid–fluid interfaces, we propose a mixed numerical method based on the MITICT. We treat the fluid–solid interfaces with the moving Lagrangian interface technique (MLIT) [28, 29] and the fluid–fluid interfaces with the ETILT. Both techniques are non-moving mesh finite element methods. In this context, the equation of motion for a rigid particle is recovered by using a high-viscosity value in the solid region.

In Section 2, we provide the governing equations. The interface update techniques are briefly described in Section 3. In Section 4, we test the mixed technique in computation of a fluid–particle interaction problem in the presence of a fluid–fluid interface. In Section 5, we present our concluding remarks.

2. GOVERNING EQUATIONS

The Navier–Stokes equations of unsteady incompressible flows are written as

$$\rho \frac{\partial \mathbf{u}}{\partial \mathrm{t}} + \rho \mathbf{u} \nabla \cdot \mathbf{u} + \nabla \mathrm{p} - \nabla \cdot (2\mu \boldsymbol{\varepsilon}) = \rho \mathbf{g} \quad \text{in } \Omega \times \mathrm{Y} \tag{1}$$

$$\nabla \cdot \mathbf{u} = 0 \quad \text{in } \Omega \times \mathrm{Y} \tag{2}$$

DOI: 10.1002/fld

where ρ, $\mathbf{u}$, p, μ, $\boldsymbol{\varepsilon}$ and $\mathbf{g}$ are the density, velocity, pressure, dynamic viscosity, strain-rate tensor, and the gravity. In these equations, Ω is the spatial domain with a smooth boundary Γ and Y is the temporal domain. This system of equations is complemented with a set of initial and boundary conditions:

$$\mathbf{u} = \mathbf{u}_0 \quad \text{in } \Omega \tag{3}$$

$$\mathbf{u} = \overline{\mathbf{u}} \quad \text{in } \Gamma_u \times \mathrm{Y} \tag{4}$$

$$\sigma \cdot \mathbf{n} = \mathbf{h} \quad \text{in } \Gamma_h \times Y \tag{5}$$

where $\mathbf{u}_0$ is the initial value of the velocity field, $\overline{\mathbf{u}}$ represents the velocity boundary condition imposed on Γ_u and $\mathbf{h}$ is the traction vector imposed over Γ_h ($\Gamma_u \cup \Gamma_h = \Gamma$ and $\Gamma_u \cap \Gamma_h = \emptyset$), typically taken as the traction-free condition: $\mathbf{h} = \mathbf{0}$.

These equations are solved over the entire spatial domain where we have one solid and two fluids ($\Omega = \Omega_s \cup \Omega_{f_1} \cup \Omega_{f_2}$). The interfaces between the different regions are determined during the computation. The motion of those interfaces and assignment (i.e. distribution) of the material properties in different regions of the domain are coupled with the solution of Equations (1) and (2). In Section 3, we describe the techniques used in calculating the evolution of the fluid–solid and fluid–fluid interfaces.

The Navier–Stokes equations are discretized with the finite element method and the generalized streamline operator technique [30]. The stabilized nature of the technique allows the use of equal-order interpolation functions for velocity and pressure. In the context of flow analysis with moving interfaces, all the element-level matrices and vectors are computed by taking into account the discontinuities in the material properties. The time integration is performed using a standard backward-Euler scheme.

3. INTERFACE UPDATE

In our numerical model based on the MITICT [16], we handle the fluid–solid interfaces with the MLIT [28, 29] and the fluid–fluid interfaces with the ETILT [16, 26, 27]. The MLIT was shown in [28, 29] to be robust in preserving the interface geometry, with the numerical results also showing independence from the element and time-step sizes. These features are important in the accurate representation of the fluid–solid interface, because despite the large displacements of the interface points, we need to preserve the interface geometry. The MLIT performs very well in that respect. The ETILT, on the other hand, is capable of representing the fluid–fluid interfaces in a robust fashion, even when those interfaces undergo large distortions.

We mix the MLIT and ETILT as follows:

1. The MLIT has priority in the motion of the fluid–solid interface and the distribution of the material properties. We assume a rigid-body motion for the solid. The volume occupied by the rigid body and its shape do not change. The material properties are distributed in the solid and fluid (including Fluids 1 and 2) regions according to the boundaries defined by the fluid–solid and fluid–fluid interfaces.
2. The ETILT needs to recognize the fluid–solid interface described by the MLIT. In the fluid, the property distribution is governed by the ETILT but the body is immersed in either Fluid

DOI: 10.1002/fld

1 or Fluid 2, or both. As the fluid–fluid interface is updated after moving the fluid–solid interface, it is necessary to avoid overlap between the solid and the new fluid distribution and, in addition, to preserve the volume in chunks of Fluids 1 and 2.

The main aspects of these techniques are briefly described below, together with some details on how the MLIT and ETILT are coupled.

3.1. Fluid–solid interface

The fluid–solid interface is defined by a collection of points that serve as markers. The motion of that material front is described by updating the markers' positions according to a simple Lagrangian scheme:

$$\mathbf{X}^{t+\Delta t} = \mathbf{X}^t + \Delta t \mathbf{V}^{t+\alpha\Delta t} \tag{6}$$

where Δt is the time step, α is the time integration parameter (usually set to 1.0), $\mathbf{X}^t$ is the known vector of markers' positions at time t, $\mathbf{X}^{t+\Delta t}$ is the updated position at time $t+\Delta t$ and $\mathbf{V}^{t+\alpha\Delta t}$ is the velocity of the markers. To avoid loss of mass during the interface evolution, a global mass correction algorithm is combined with the solution of Equation (6). Material properties are assigned at integration-point level, depending on what side of the interface the integration point belongs to. To capture the discontinuity in material properties, the elements crossed by the interface are subdivided to have higher-resolution integration. The integration strategy adopted in this work consists in subdividing the element parent domain by taking uniform length subintervals in each space direction (in practice, three partitions in each direction are used). No regularization is needed in this field. Details and numerical evaluation of the MLIT can be found in [28, 29].

3.2. Fluid–fluid interface

To identify the interface between the two fluids, a Heaviside function H is used. In the discrete space, an indicator along the edges of the elements crossed by the interface can be used to define the interface position. In the ETILT, $\varphi^{he} = H(\varphi^h(\mathbf{x}_f) - Z)$, where φ^{he} is the edge-based representation of the interface, $\mathbf{x}_f$ is the interface position, and φ^h is the nodal representation of φ. Any value of Z within the interval [0,1] could be considered provided that all the steps involved in the ETILT be consistently performed with such a value [26, 27]. Here, the choice $Z = 0.5$ is adopted to mark the interface. In this context, φ^h is computed by using a constrained least-squares projection [27, 31, 32]:

$$\int_\Omega \psi^h(\varphi_n^h - \varphi_n^{he})\,\mathrm{d}\Omega + \sum_{k=1}^{n_{ie}} \psi^h(\mathbf{x}_k)\lambda_{\mathrm{PEN}}(\varphi_n^h(\mathbf{x}_k) - 0.5) = 0 \tag{7}$$

where ψ^h is the test function, n_{ie} is the number of element edges crossed by the interface, $\mathbf{x}_k$ is the coordinate of the interface location along the kth edge, and λ_{PEN} is a penalty parameter. The penalty parameter ensures that the projection topologically preserves the interface position along the edges. In four-noded quadrilateral elements, this condition is activated also along the element diagonals crossed by the interface. After this projection, to compute φ_{n+1}^h, i.e. φ^h at time level $n+1$, we use a discrete formulation of the advection equation based on the streamline upwind/Petrov–Galerkin (SUPG) formulation [33] with the Crank–Nicholson time integration scheme. From φ_{n+1}^h we obtain φ_{n+1}^{he} by a combination of a least-squares projection and corrections to enforce volume

DOI: 10.1002/fld

conservation for chunks of Fluids 1 and 2. At each time step, a property P is interpolated as follows:

$$P^h = \varphi^{he} P_1 + (1 - \varphi^{he}) P_2 \tag{8}$$

As in the MLIT, the elements crossed by the interface are integrated with higher-resolution integration to capture the discontinuity in material properties, and no regularization is needed in the P field. Details and numerical evaluation of the ETILT can be found in [26, 27].

Remark
In the present study, φ^{he}_{n+1} must additionally identify the rigid zone, i.e. the fluid–solid interface. This means that the condition $(\varphi^h_{n+1} - 0.5) = 0$ needs be strongly satisfied for points belonging to that interface. To this end, the edges crossed by the Lagrangian fluid–solid interface are added to the summation in Equation (7). Moreover, as the rigid-body motion has priority and the computation *via* the MLIT ensures the volume preservation in the solid, the ETILT corrections in φ^{he}_{n+1} to enforce volume conservation are not used along the fluid–solid interface. This strategy handles the overlap in the zone of action of the two methods when the rigid body is simultaneously in touch with Fluids 1 and 2.

4. TEST COMPUTATION

In this test computation, we have a Nylon sphere falling in a fluid-filled tube, where the upper part of the tube is occupied by a fluid representing the air, and the lower part by a fluid representing silicon oil (see Figure 1). The sphere first falls through the air, then it impacts the oil surface, and then it falls through the oil. Experimental investigation of a Nylon sphere settling in oil is reported in [34]. Although the air–oil interface was not reported in that reference, the terminal velocity of the sphere was. We compare that to the terminal velocity we obtain from our computations.

4.1. Computational result

The material properties for the Nylon sphere and silicon oil are $\rho_s = 1120\,\mathrm{kg/m^3}$, $\rho_{l_1} = 962\,\mathrm{kg/m^3}$ and $\mu_{l_1} = 0.113\,\mathrm{kg/m/s}$. The diameter of the sphere is $d = 15\,\mathrm{mm}$, and the tube has a diameter $D = 100\,\mathrm{mm}$ and length $L = 160\,\mathrm{mm}$. Initially the lowest point of the sphere is at $H = 120\,\mathrm{mm}$. These properties and dimensions were taken from [34]. The material properties used for the air are $\rho_{l_2} = 1\,\mathrm{kg/m^3}$ and $\mu_{l_2} = 0.001\,\mathrm{kg/m/s}$. Initially the oil surface is at $F = 88\,\mathrm{mm}$ from the bottom of the tube. A large viscosity value of $\mu_s = 10^7\,\mathrm{kg/m/s}$ is used for the solid region to mimic, in the context of the present formulation, the rigid behaviour of the sphere. The time-step size is fixed at 0.001 s and is basically determined from the ETILT requirements. Because the Reynolds number is rather low ($Re = 11.6$) in this case, three-dimensional effects are not reported experimentally. This allows us to use an axisymmetric model in the computation. The motion is governed by gravity ($g = 9.8\,\mathrm{m/s^2}$), buoyancy and viscous stresses.

Figure 2 shows the oil surface and the sphere at different instants. Because the viscosity of the oil is rather high, the free surface is smooth. Figure 3 shows the time evolution of the position of the sphere and its velocity. The particle motion is governed by the gravity ($V = gt$) until about $t = 0.08$ s, at which time the sphere reaches the oil surface (as can also be seen in Figure 2). The time it takes the sphere to reach the oil surface can of course also be estimated from $t = (2l/g)^{1/2}$,

DOI: 10.1002/fld

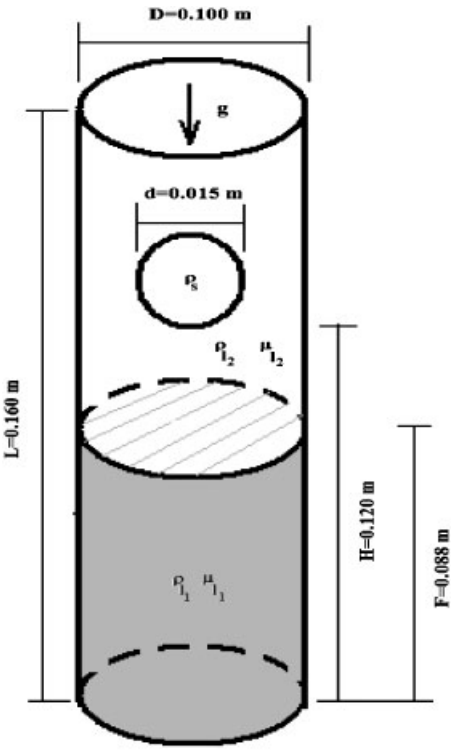

Figure 1. A sphere falling in a tube with two different viscous fluids.

with $l = 0.032$ m being the initial distance between the sphere and the oil surface. After that a transition period is seen, indicative of the interaction between the sphere and the oil surface. Following that a terminal velocity $V_t = 0.08$ m/s is reached, and this value compares well with the measured value reported in [34]. Finally, the velocity of the sphere becomes zero as it settles at the bottom of the tube.

4.2. Comparison to analytical prediction

The terminal velocity of the sphere can also be predicted analytically based on the balance of the forces acting on an immersed sphere:

$$F_g - F_b - F_D = 0 \tag{9}$$

where F_g, F_b and F_D are the weight of the sphere, the buoyancy force and the drag force, respectively, with the following well-known expressions:

$$F_g = \rho_s g \pi d^3/6 \tag{10a}$$

$$F_b = \rho_l g \pi d^3/6 \tag{10b}$$

$$F_D = C_D \rho_l \pi d^2/8 V_t^2 \tag{10c}$$

DOI: 10.1002/fld

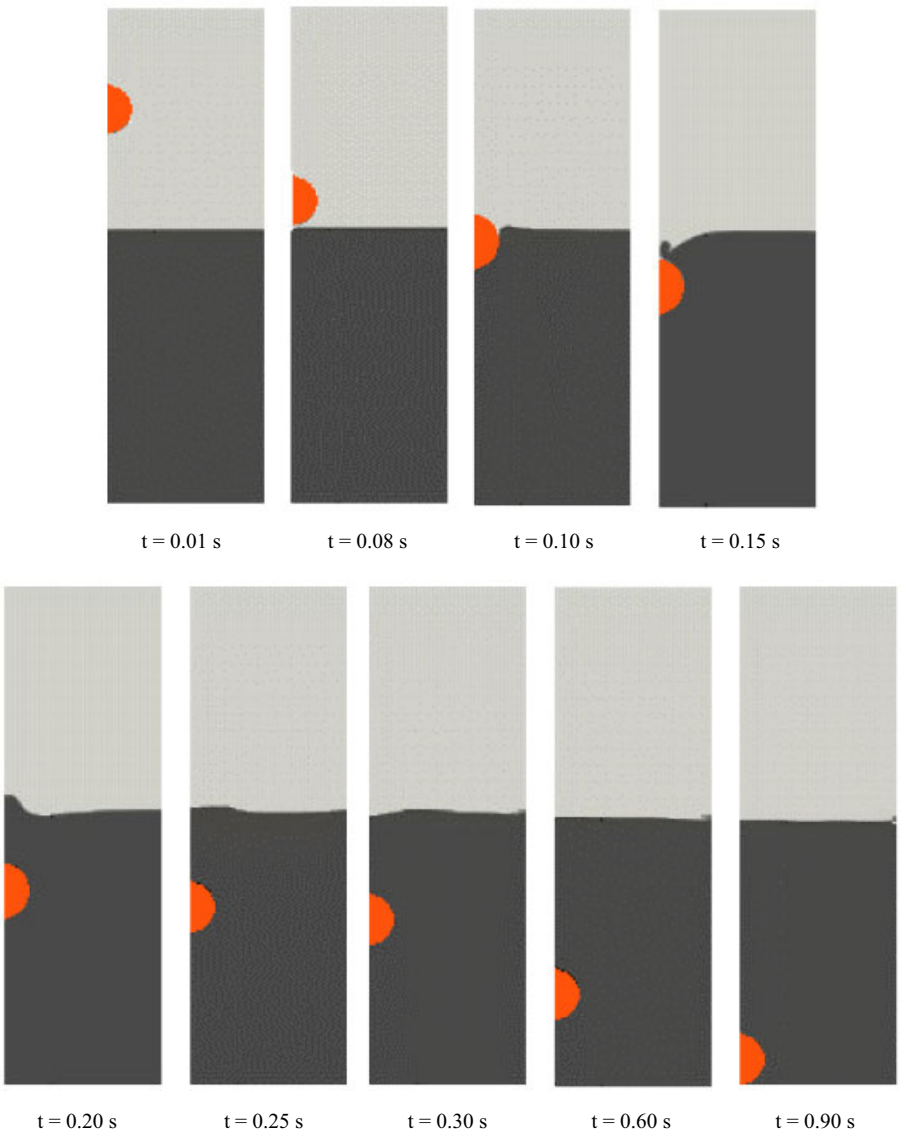

Figure 2. A sphere falling in a tube with two different viscous fluids. The fluid–fluid interface and the sphere at different instants.

The drag coefficient C_D depends on the Reynolds number, with the relationship known from experiments for a sphere in infinite domain, without the wall effects. For the range of Reynolds numbers we are working with, the expression for the drag coefficient is given [35, 36] as

$$C_D = 27.33\, Re^{-0.764} \tag{11}$$

DOI: 10.1002/fld

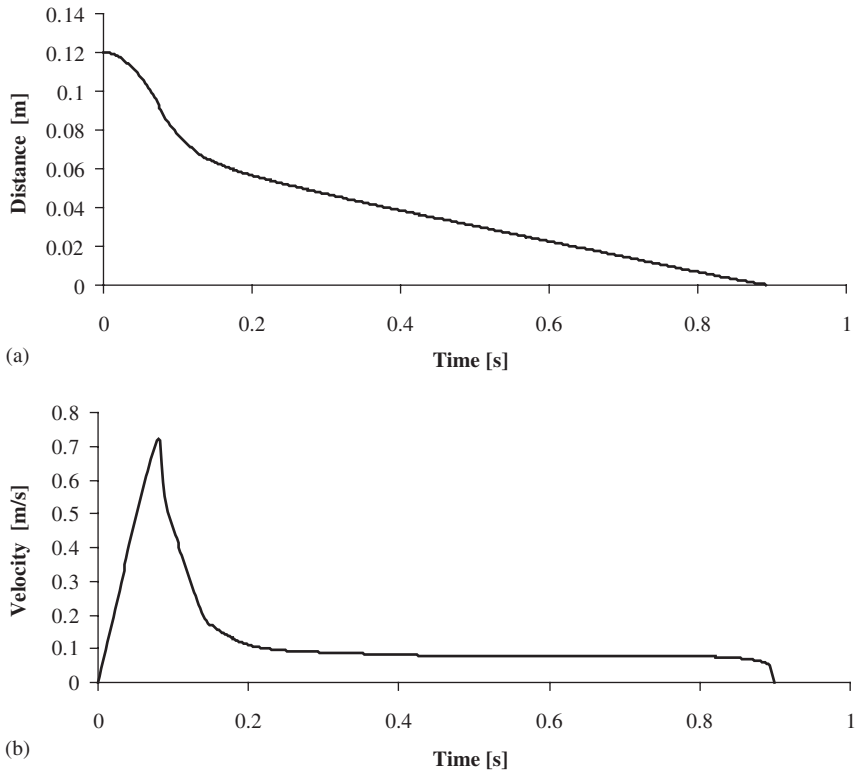

Figure 3. A sphere falling in a tube with two different viscous fluids. Time evolution of: (a) the position of the sphere and (b) its velocity.

From Equations (9)–(11), the terminal velocity, without the wall effects, can be calculated as $U = 0.0857\,\mathrm{m/s}$. In the computation, as well as in the experiment, the terminal velocity is affected by the walls of the tube, hence U needs to be adjusted using a correction factor $f = V_t/U = 1-(d/D)^{3/2}$ [35], resulting in a value $V_t = 0.0807\,\mathrm{m/s}$. The computed value is in close agreement with this.

5. CONCLUDING REMARKS

We proposed a mixed numerical model for computation of flow problems where both fluid–solid and fluid–fluid interfaces are present. The model is based on the MITICT introduced earlier. In the MITICT, fluid–solid interfaces are accurately tracked with a moving mesh method. Fluid–fluid interfaces, if they are too complex and unsteady to follow with a mesh, are represented with an interface-capturing technique, using non-moving meshes. In the numerical model we presented here, fluid–solid interfaces are treated with the MLIT and fluid–fluid interfaces with the ETILT. The two components of the mixed method both have desirable properties, suitable for the type of interfaces they are used for. The MLIT is robust in preserving the interface geometry and its

DOI: 10.1002/fld

performance is rather independent from the element and time-step sizes. The ETILT does well in representing the fluid–fluid interfaces in a robust fashion, even when those interfaces undergo large distortions.

We tested the model on computation of the fluid–particle interactions seen when a sphere falls in a tube filled with two different fluids. This includes the interaction between the sphere and the fluid–fluid interface as the sphere crosses from one fluid region to other. To an extent limited by the availability of the experimental data and analytical predictions, we compared the computed results with those obtained experimentally and predicted analytically. These limited comparisons, based on the terminal velocity of the sphere, show that the computed results are in close agreement with the experimental and analytical results.

ACKNOWLEDGEMENTS

The support provided by the Chilean Council of Research and Technology CONICYT (FONDECYT Project No. 1060141) and the Department of Technological and Scientific Research at the University of Santiago de Chile (DICYT-USACH) is gratefully acknowledged.

REFERENCES

1. Hughes TJR, Liu WK, Zimmermann TK. Lagrangian–Eulerian finite element formulation for incompressible viscous flows. *Computer Methods in Applied Mechanics and Engineering* 1981; **29**:239–349.
2. Huerta A, Liu W. Viscous flow with large free surface motion. *Computer Methods in Applied Mechanics and Engineering* 1988; **69**:277–324.
3. Sarrate J, Huerta A, Donea J. Arbitrary Lagrangian–Eulerian formulation for fluid-rigid body interaction. *Computer Methods in Applied Mechanics and Engineering* 2001; **190**:3171–3188.
4. Khurram RA, Masud A. A multiscale/stabilized formulation of the incompressible Navier–Stokes equations for moving boundary flows and fluid–structure interaction. *Computational Mechanics* 2006; **38**:403–416.
5. Masud A. Effects of mesh motion on the stability and convergence of ALE based formulations for moving boundary flows. *Computational Mechanics* 2006; **38**:430–439.
6. Bazilevs Y, Calo VM, Zhang Y, Hughes TJR. Isogeometric fluid–structure interaction analysis with applications to arterial blood flow. *Computational Mechanics* 2006; **38**:310–322.
7. Masud A, Hughes TJR. A space-time Galerkin/least-squares finite element formulation of the Navier–Stokes equations for moving domain problems. *Computer Methods in Applied Mechanics and Engineering* 1997; **146**:91–126.
8. Tezduyar TE. Stabilized finite element formulations for incompressible flow computations. *Advances in Applied Mechanics* 1992; **28**:1–44.
9. Tezduyar TE, Behr M, Liu J. A new strategy for finite element computations involving moving boundaries and interfaces—the deforming-spatial-domain/space–time procedure: I. The concept and the preliminary numerical tests. *Computer Methods in Applied Mechanics and Engineering* 1992; **94**:339–351.
10. Tezduyar TE, Behr M, Mittal S, Liu J. A new strategy for finite element computations involving moving boundaries and interfaces—the deforming-spatial-domain/space–time procedure: II. Computation of free-surfaces flows, two-liquid flows, and flows with drifting cylinders. *Computer Methods in Applied Mechanics and Engineering* 1992; **94**:353–371.
11. Tezduyar TE. Computation of moving boundaries and interfaces and stabilization parameters. *International Journal for Numerical Methods in Fluids* 2003; **43**:555–575.
12. Tezduyar T, Aliabadi S, Behr M, Johnson A, Mittal S. Parallel finite element computation of 3D flows. *Computer* 1993; **26**:27–36.
13. Tezduyar TE, Aliabadi SK, Behr M, Mittal S. Massively parallel finite element simulation of compressible and incompressible flows. *Computer Methods in Applied Mechanics and Engineering* 1994; **119**:157–177.
14. Mittal S, Tezduyar TE. Parallel finite element simulation of 3D incompressible flows—Fluid–structure interactions. *International Journal for Numerical Methods in Fluids* 1995; **21**:933–953.

DOI: 10.1002/fld

15. Tezduyar T, Aliabadi S, Behr M, Jonson A, Kalro V, Litke M. Flow simulation and high performance computing. *Computational Mechanics* 1996; **18**:397–412.
16. Tezduyar TE. Finite element methods for flow problems with moving boundaries and interfaces. *Archives of Computational Methods in Engineering* 2001; **8**:83–130.
17. Tezduyar TE, Sathe S, Keedy R, Stein K. Space–time finite element techniques for computation of fluid–structure interactions. *Computer Methods in Applied Mechanics and Engineering* 2006; **195**:2002–2027.
18. Kuttler U, Forster C, Wall WA. A solution for the incompressibility dilemma in partitioned fluid–structure interaction with pure Dirichlet fluid domains. *Computational Mechanics* 2006; **38**:417–429.
19. Dettmer W, Peric D. A computational framework for fluid–rigid body interaction: finite element formulation and applications. *Computer Methods in Applied Mechanics and Engineering* 2006; **195**:1633–1666.
20. Masud A, Bhanabhagvanwala M, Khurram RA. An adaptive mesh rezoning scheme for moving boundary flows and fluid–structure interaction. *Computers and Fluids* 2007; **36**:77–91.
21. Sawada T, Hisada T. Fluid–structure interaction analysis of the two dimensional flag-in-wind problem by an interface tracking ALE finite element method. *Computers and Fluids* 2007; **36**:136–146.
22. Tezduyar T, Aliabadi S, Behr M. Enhanced-discretization interface-capturing technique (EDICT) for computation of unsteady flows with interfaces. *Computer Methods in Applied Mechanics and Engineering* 1998; **155**:235–248.
23. Wagner GJ, Moës N, Liu WK, Belytschko T. The extended finite element methods for rigid particles in Stokes flow. *International Journal for Numerical Methods in Engineering* 2001; **51**:293–313.
24. Peskin AP, Hardin GR. Moving particles through a finite element mesh. *Journal of Research of the National Institute of Standards and Technology* 1998; **103**:77–91.
25. Akin JE, Tezduyar TE, Ungor M. Computation of flow problems with the mixed interface-tracking/interface-capturing technique (MITICT). *Computers and Fluids* 2007; **36**:2–11.
26. Cruchaga MA, Celentano DJ, Tezduyar TE. Moving-interface computations with the edge-tracked interface locator technique (ETILT). *International Journal for Numerical Methods in Fluids* 2005; **47**:451–469.
27. Cruchaga MA, Celentano DJ, Tezduyar TE. Collapse of a liquid column: numerical simulation and experimental validation. *Computational Mechanics* 2007; **39**:453–476.
28. Cruchaga M, Celentano D, Tezduyar T. A moving Lagrangian interface technique for flow computations over fixed meshes. *Computer Methods for Applied Mechanics and Engineering* 2001; **191**:525–543.
29. Cruchaga M, Celentano D, Tezduyar T. Computation of mould filling processes with a moving Lagrangian interface technique. *Communications in Numerical Methods in Engineering* 2002; **18**:483–493.
30. Cruchaga MA, Oñate E. A generalized streamline finite element approach for the analysis of incompressible flow problems including moving surfaces. *Computer Methods in Applied Mechanics and Engineering* 1999; **173**:241–255.
31. Tezduyar TE. Finite elements methods for fluid dynamics with moving boundaries and interfaces. In *Encyclopedia of Computational Mechanics*, *Volume 3*: *Fluids*, Chapter 17, Stein E, De Borst R, Hughes TJR (eds). Wiley: New York, 2004.
32. Tezduyar TE. Interface-tracking and interface-capturing techniques for finite element computation of moving boundaries and interfaces. *Computer Methods in Applied Mechanics and Engineering* 2006; **195**:2983–3000.
33. Brooks AN, Hughes TJR. Streamline upwind/Petrov–Galerkin formulations for convection dominated flows with particular emphasis on the incompressible Navier–Stokes equations. *Computer Methods in Applied Mechanics and Engineering* 1982; **32**:199–259.
34. ten Cate A, Nieuwstad CH, Derksen JJ, Van den Akker HEA. Particle imaging velocimetry experiments and lattice-Boltzmann simulations on a single sphere settling under gravity. *Physics of Fluids* 2002; **14**:4012–4025.
35. White FM. *Viscous Fluid Flow*. McGraw-Hill: New York, 2005.
36. Chhabra RP, Agarwal S, Chaudhary K. A note on wall effect on the terminal falling velocity of a sphere in quiescent Newtonian media in cylindrical tubes. *Powder Technology* 2003; **129**:53–58.

DOI: 10.1002/fld